JM FOCUS ON FLUIDS

From classical to ultimate heat fluxes for convection at a vertical wall

Andrew J. Wells†

Atmospheric, Oceanic and Planetary Physics, Department of Physics, University of Oxford, Oxford OX1 3PU, UK

Convection from a buoyancy source distributed over a vertical wall has diverse applications, from the natural ventilation of buildings to the melting of marine-terminating glaciers which impacts on future sea level. A key challenge involves determining how the rate and mechanisms of turbulent heat transfer should be extrapolated across a range of scales. Ke *et al.* (*J. Fluid Mech.*, vol. 964, 2023, A24) explore transitions in the turbulent flow dynamics using direct numerical simulation of a convective boundary layer at a heated vertical wall. A classical regime of heat transfer, consistent with previous laboratory experiments, gives way with increasing accumulation of buoyancy to an ultimate regime with enhanced heat transfer. The key to this transition lies in a near-wall sublayer, with a switch from laminar buoyancy-driven dynamics to a sublayer dominated by turbulence and shear instability from the mean flow.

Key words: turbulent boundary layers

1. Introduction

Turbulent buoyant convection of fluid heated by a vertical wall is a classic fluid mechanics problem, for example seen when hot air rises next to the front of a convective heater used to warm an office or room. Whilst much early work on this problem was driven by engineering applications to industrial heating or cooling, the dynamics of these so-called vertical natural convection boundary layers is of contemporary relevance to diagnosing the impacts of climate change, and mitigation strategies from energy-efficient design. The ventilation and environmental comfort of buildings in which we live and work can be moderated by flows induced by warm, buoyant air rising near a hot wall of a building, or cold air sinking (e.g. Linden 1999; Bonnebaigt, Caulfield & Linden 2018). Meanwhile, in Greenland and Antarctica the melting of steep glacier termini releases fresh and buoyant meltwater into the ocean, driving convective flow and enhancing heat transfer to the ice. Such convective boundary layers impact how ice sheets discharge ice mass and thus how

† Email address for correspondence: andrew.wells@physics.ox.ac.uk

sea levels respond to changing ocean temperatures (see reviews by Straneo & Cenedese 2015; Malyarenko *et al.* 2020). The freshwater release also impacts ocean circulation and nutrient supply for marine ecological blooms.

As with many convection problems, it is important to understand how results from laboratory-scale experiments and state-of-the-art numerical simulations might be extrapolated to the more extreme scales present in some applications. For thermally driven convective flows, the magnitude of buoyant driving versus dissipation can be described by a Rayleigh number, $Ra = g\alpha\Delta T L^3/\kappa\nu$, written in terms of the gravitational acceleration g, imposed temperature difference ΔT, thermal expansion coefficient α, thermal diffusivity κ, kinematic viscosity ν and characteristic length scale L. Flows are alternatively characterised via a Grashof number $Gr = Ra/Pr$ and Prandtl number $Pr = \nu/\kappa$. There has been considerable interest in understanding how key properties such as the dimensionless heat flux, or Nusselt number $Nu = qL/k\Delta T$, vary with Ra for turbulent flow (where q is the heat flux from the wall and k the thermal conductivity). The key mechanisms have been debated at length for the related problem of Rayleigh–Bénard convection between hot and cold horizontal boundaries (Ahlers, Grossmann & Lohse 2009), where the boundary layers at the walls play a key role. Different theories for a classical regime feature the key ingredients of predominantly laminar boundary layers with the occasional buoyant detachment of plumes (see e.g. Howard 1966; Grossmann & Lohse 2001, 2011), and predict scalings $Nu \propto Ra^\alpha$ with $\alpha \leq 1/3$ for moderate Pr. However, for large enough Ra, the turbulent interior generates mean flows along the boundary that are sufficient for the boundary layers to become turbulent and dominated by shear (Kraichnan 1962; Grossmann & Lohse 2011). In this latter so-called ultimate regime, the heat flux is more efficient with an asymptotic $Nu \propto Ra^{1/2}$ scaling predicted as $Ra \to \infty$ (to within logarithmic corrections, which lead to apparent scaling exponents $1/3 < \alpha \leq 1/2$ for the range of Ra currently accessible in laboratory experiment or simulation).

The above dynamics finds a natural home for convective boundary layers at vertical walls, where buoyancy directly generates a mean flow along the walls. Early experiments and simulations with buoyancy supplied by a single vertical wall (see Papailiou (1991), Kerr & McConnochie (2015), Nakao, Hattori & Suto (2017) and references therein) are consistent with a classical scaling $Nu \propto Ra^{1/3}$, and with theories for a buoyancy-driven sublayer near the wall (George & Capp 1979; Hölling & Herwig 2005; Wells & Worster 2008). But shear-dominated dynamics has been hypothesised for vertical boundary layers at large Ra (Wells & Worster 2008), building on ideas for the ultimate regime of Rayleigh–Bénard convection. For convective channel flow between hot and cold vertical boundaries, hints of incipient ultimate-regime behaviour are seen from statistics conditionally averaged over regions of high shear (Ng *et al.* 2017). A transition to shear-dominated heat transfer is also seen in experiments that inject a buoyant plume to supplement a convective boundary layer (McConnochie & Kerr 2017). But how might the shear-dominated regime develop for convection at a single heated wall? Beyond its fundamental interest, this question has important implications: extrapolating classical and ultimate regime scalings to the geophysical scale of a glacier terminus can lead to predicted melt rates differing by a factor of up to 10 (Wells & Worster 2008).

2. Overview

Ke *et al.* (2023) explore the mechanisms for the regime transition in turbulent boundary-layer dynamics for a transiently developing flow from a heated wall. They consider a vertically periodic numerical domain, building on their previous direct
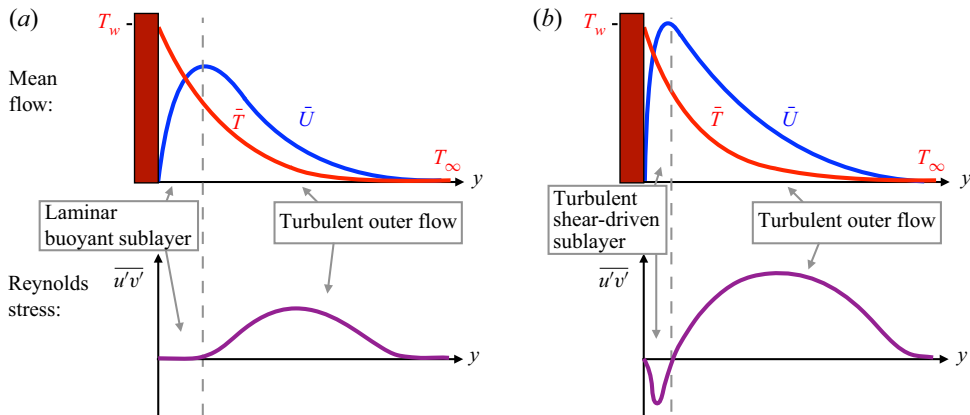
Figure 1. Schematic of mean profiles of vertical velocity $\bar{U}$ and temperature $\bar{T}$ varying with distance y from the wall (upper row) and Reynolds stresses $\overline{u'v'}$ (lower row) for convection from a wall at hotter temperature T_w than the far-field temperature T_∞. (a) Classical regime and (b) ultimate regime.

numerical simulations of this configuration (Ke *et al.* 2020, 2021). Identifying the length scale L with the boundary-layer thickness, this suite of simulations suggests that the dimensionless heat flux scales as $Nu \propto Gr^{1/3} \propto Ra^{1/3}$ for intermediate Gr, consistent with previous scalings in the classical regime. However, $Nu \propto Gr^{0.381}$ for $10^7 \leq Gr \leq 10^8$, consistent with ultimate-regime heat transfer with logarithmic corrections.

By probing the underlying differences in boundary-layer structure, Ke *et al.* (2023) provide further evidence to support this suggestion of the ultimate heat-transfer scaling, with a key role for inner and outer shear layers in the mean flow along the wall (see figure 1). For the classical regime at intermediate Gr, shear production dominates the turbulent kinetic energy budget in the outer shear layer, but with low turbulent production in a relatively laminar near-wall shear layer. The buoyancy flux from the wall plays a key role in driving the mean flow, but appears less significant in the production of turbulent kinetic energy. Transitioning into the ultimate regime, a second peak of turbulent kinetic energy develops in the inner shear layer with enhanced shear production and the growth of turbulent Reynolds stresses in this inner region. Several features develop that are commonly seen in pure shear flows. Longitudinal streaks develop in the near-wall region for large Gr, with a wavelength commensurate with that observed for canonical turbulent shear flows. The wall drag coefficient transitions from a laminar scaling to one consistent with a turbulent logarithmic layer, coincident with a transition in estimated viscous sublayer thickness. The usual logarithmic profile of velocity in a shear flow is, however, modified to account for buoyancy from a logarithmic variation of mean temperature, and the ratio of turbulent production to dissipation is larger than for a pure shear flow. The combined package provides evidence of a transition from a classical heat-transfer regime with an inner laminar flow driven by buoyancy to an ultimate heat-transfer regime where shear-driven instabilities generate a turbulent inner region of the boundary layer.

3. Future

The mechanistic evidence of a regime transition presented by Ke *et al.* (2023) provides insight to guide the description of convective boundary-layer processes at more extreme scales. Many ice-sheet and ocean models exploit heat transfer scalings consistent with a shear-controlled ultimate regime (Malyarenko *et al.* 2020), but for convective flows at steep

ice faces this will only be accurate after sufficient flow develops to exceed the transitional value of *Gr*. Whilst one would expect a similar pattern of flow dynamics, an immediate query is whether the transitional *Gr* for transiently developing flow with translation symmetry will apply directly to spatially developing flows with along-flow gradients. Ice melting in salty ocean water also features two-component flow with Prandtl and Schmidt numbers much larger than the value, $Pr = 0.71$, considered by Ke *et al.* (2023), which will impact boundary-layer development (Howland, Verzicco & Lohse 2023). A further factor for glacial melting is the ocean density stratification, which can generate layering of the flow (Huppert & Turner 1978) or detrainment from the boundary layer (Bonnebaigt *et al.* 2018). Such detrainment can also be relevant to convection through thermal gradients in building ventilation (Bonnebaigt *et al.* 2018).

For engineering applications, the results presented by Ke *et al.* (2023) may offer insight into flow control strategies to optimise heat transfer. The ultimate regime has higher efficiency of heat transfer and appears to arise from instability and the production of turbulence in the inner shear layer in the near-wall flow. This instability might be manipulated to promote or delay the transition to the ultimate regime. The detailed investigation of the transition from the classical to ultimate regime by Ke *et al.* (2023) offers potential for improved characterisation and control of vertical natural convection boundary layers.

Author ORCIDs.
Andrew J. Wells https://orcid.org/0000-0001-7929-6227.

REFERENCES

AHLERS, G., GROSSMANN, S. & LOHSE, D. 2009 Heat transfer and large scale dynamics in turbulent Rayleigh–Bénard convection. *Rev. Mod. Phys.* **81** (2), 503–537.

BONNEBAIGT, R., CAULFIELD, C.P. & LINDEN, P.F. 2018 Detrainment of plumes from vertically distributed sources. *Environ. Fluid Mech.* **18** (1), 3–25.

GEORGE, W.K. & CAPP, S.P. 1979 A theory for natural convection turbulent boundary layers next to heated vertical surfaces. *Intl J. Heat Mass Transfer* **22**, 813–826.

GROSSMANN, S. & LOHSE, D. 2001 Thermal convection for large Prandtl numbers. *Phys. Rev. Lett.* **86** (15), 3316–3319.

GROSSMANN, S. & LOHSE, D. 2011 Multiple scaling in the ultimate regime of thermal convection. *Phys. Fluids* **23** (4), 045108.

HÖLLING, M. & HERWIG, H. 2005 Asymptotic analysis of the near-wall region of turbulent natural convection flows. *J. Fluid Mech.* **541**, 383–397.

HOWARD, L.N. 1966 Convection at high Rayleigh number. In *Applied Mechanics, Proceedings of the 11th Congress of Applied Mechanics Munich (Germany)* (ed. H. Görtler), pp. 1109–1115. Springer.

HOWLAND, C.J., VERZICCO, R. & LOHSE, D. 2023 Double-diffusive transport in multicomponent vertical convection. *Phys. Rev. Fluids* **8** (1), 013501.

HUPPERT, H.E. & TURNER, J.S. 1978 On melting icebergs. *Nature* **271**, 46–48.

KE, J., WILLIAMSON, N., ARMFIELD, S.W. & KOMIYA, A. 2023 The turbulence development of a vertical natural convection boundary layer. *J. Fluid Mech.* **964**, A24.

KE, J., WILLIAMSON, N., ARMFIELD, S.W., KOMIYA, A. & NORRIS, S.E. 2021 High Grashof number turbulent natural convection on an infinite vertical wall. *J. Fluid Mech.* **929**, A15.

KE, J., WILLIAMSON, N., ARMFIELD, S.W., NORRIS, S.E. & KOMIYA, A. 2020 Law of the wall for a temporally evolving vertical natural convection boundary layer. *J. Fluid Mech.* **902**, A31.

KERR, R.C. & MCCONNOCHIE, C.D. 2015 Dissolution of a vertical solid surface by turbulent compositional convection. *J. Fluid Mech.* **765**, 211–228.

KRAICHNAN, R.H. 1962 Turbulent thermal convection at arbitrary Prandtl number. *Phys. Fluids* **5** (11), 1374–1389.

LINDEN, P.F. 1999 The fluid mechanics of natural ventilation. *Annu. Rev. Fluid Mech.* **31** (1), 201–238.

MALYARENKO, A., WELLS, A.J., LANGHORNE, P.J., ROBINSON, N.J., WILLIAMS, M.J.M. & NICHOLLS, K.W. 2020 A synthesis of thermodynamic ablation at ice–ocean interfaces from theory, observations and models. *Ocean Model.* **154**, 101692.

MCCONNOCHIE, C.D. & KERR, R.C. 2017 Enhanced ablation of a vertical ice wall due to an external freshwater plume. *J. Fluid Mech.* **810**, 429–447.

NAKAO, K., HATTORI, Y. & SUTO, H. 2017 Numerical investigation of a spatially developing turbulent natural convection boundary layer along a vertical heated plate. *Intl J. Heat Fluid Flow* **63**, 128–138.

NG, C.S., OOI, A., LOHSE, D. & CHUNG, D. 2017 Changes in the boundary-layer structure at the edge of the ultimate regime in vertical natural convection. *J. Fluid Mech.* **825**, 550–572.

PAPAILIOU, D.D. 1991 Turbulence models for natural convection flows along a vertical heated plane. *Tech. Rep.* AGARD-A-R-291 4-1 to 4-5. AGARD.

STRANEO, F. & CENEDESE, C. 2015 The dynamics of Greenland's glacial fjords and their role in climate. *Annu. Rev. Mar. Sci.* **7** (1), 89–112.

WELLS, A.J. & WORSTER, M.G. 2008 A geophysical-scale model of vertical natural convection boundary layers. *J. Fluid Mech.* **609**, 111–137.